ISME

www.nature.com/ismej

ARTICLE

Mobile genetic elements used by competing coral microbial populations increase genomic plasticity

Pengxia Wang[1,2,3], Yi Zhao[4], Weiquan Wang[1,2,3], Shituan Lin[1,2,3], Kaihao Tang[1,2], Tianlang Liu[1,2,3], Thomas K. Wood[5] and Xiaoxue Wang[1,2,3]✉

© The Author(s), under exclusive licence to International Society for Microbial Ecology 2022

Intraspecies diversification and niche adaptation by members of the *Vibrio* genus, one of the most diverse bacterial genera, is thought to be driven by horizontal gene transfer. However, the intrinsic driving force of *Vibrio* species diversification is much less explored. Here, by studying two dominant and competing cohabitants of the gastric cavity of corals, we found that a phenotype influencing island (named VPII) in *Vibrio alginolyticus* was eliminated upon coculturing with *Pseudoalteromonas*. The loss of VPII reduced the biofilm formation and phage resistance, but activated motility, which may allow *V. alginolyticus* to expand to other niches. Mechanistically, we discovered that the excision of this island is mediated by the cooperation of two unrelated mobile genetic elements harbored in *Pseudoalteromonas* spp., an integrative and conjugative element (ICE) and a mobilizable genomic island (MGI). More importantly, these mobile genetic elements are widespread in cohabitating Gram-negative bacteria. Altogether, we discovered a new strategy by which the mobilome is employed by competitors to increase the genomic plasticity of rivals.

The ISME Journal; https://doi.org/10.1038/s41396-022-01272-1

INTRODUCTION

The genus *Vibrio*, one of the most diverse bacterial genera, consists of over 150 species (www.bacterio.net/vibrio.html) containing both facultative symbiotic and pathogenic strains. Some *Vibrio* species, such as *Vibrio cholerae*, *Vibrio parahaemolyticus* and *Vibrio vulnificus*, are commonly identified as causative agents of human disease. In addition, some *Vibrio* spp., such as *Vibrio coralliilyticus, Vibrio shilonii* and *Vibrio alginolyticus*, are capable of infecting fish, corals, and other marine invertebrates [1]. Members of the *Vibrio* genus occupy habitats ranging from freshwater to the deep sea, as well as associate with various eukaryotes [1, 2]. The ecological diversity of this genus may be attributed, in part, to the acquisition of mobile genetic elements. Furthermore, mobile genetic elements may contribute to niche adaptation, as demonstrated for some environmental *Vibrio* spp., and may eventually lead to speciation (Hunt et al., 2008). Their short generation time gives many *Vibrio* spp. a fitness advantage. Moreover, many *Vibrio* species form robust biofilms on both biotic and abiotic surfaces, which plays an essential role in their environmental persistence [1]. These features of *Vibrio* spp. and the complete genomes of closely related species from various aquatic niches make this group an excellent case study for prokaryotic genome evolution and adaptation.

Vibrio spp. are prevalent in the coral microbiome, and coral health is inversely related to the abundance of *Vibrio* species [3]. Prokaryote-prokaryote interactions are frequent and can affect the composition and ecological function of the coral microbiome. *Pseudoalteromonas* spp. are also commonly found in corals [4, 5] and are regarded as competitors of *Vibrio* spp. since members of these two genera compete for the same resources [6–8]. Competition between *Pseudoalteromonas* and *Vibrio* species includes secreting active compounds for direct killing, inhibiting quorum sensing, and interfering with biofilm formation [9–11]. *Pseudoalteromonas* species are thus utilized in coral probiotics against *Vibrio* spp [12, 13].

Here, by studying *Vibrio* spp. and *Pseudoalteromonas* spp. cohabiting the gastric cavity of coral, we found that *V. alginolyticus* generates variants with altered surface colonization and phage resistance when cocultured with *Pseudoalteromonas* spp. Mechanistically, we discovered that the mobilome, the pool of mobile genetic elements in the microbiome, is responsible for the genetic variation in *V. alginolyticus*. Specifically, we demonstrate that the tight cooperative action of two mobile genetic elements from *Pseudoalteromonas* spp., an integrative and conjugative element (ICE) and a mobilizable genomic island (MGI), triggers the excision of an important "phenotype influencing island", VPII, in *V. alginolyticus*. Through deletion and complementation studies, the loss of VPII in *V. alginolyticus* leads to an increase in swimming motility and a corresponding decrease in biofilm formation and phage resistance. Thus, the mobilome is a powerful molecular tool for rapidly promoting niche adaptation and genetic diversification of *Vibrio* species. Furthermore, our analysis revealed that the cooccurrence of ICEs, MGIs and VPII is ubiquitous in bacteria, indicating that the cooperative action of mobile genetic elements

[1]Key Laboratory of Tropical Marine Bio-resources and Ecology, Guangdong Key Laboratory of Marine Materia Medica, Innovation Academy of South China Sea Ecology and Environmental Engineering, South China Sea Institute of Oceanology, Chinese Academy of Sciences, 164 West Xingang Road, Guangzhou 510301, China. [2]Southern Marine Science and Engineering Guangdong Laboratory (Guangzhou), No.1119, Haibin Road, Nansha District, Guangzhou 511458, China. [3]University of Chinese Academy of Sciences, Beijing 100049, China. [4]College of Life Sciences, Hebei Normal University, Shijiazhuang 050024 Hebei, China. [5]Department of Chemical Engineering, Pennsylvania State University, University Park, PA 16802-4400, USA. ✉email: xxwang@scsio.ac.cn

Received: 12 January 2022 Revised: 30 May 2022 Accepted: 15 June 2022
Published online: 27 June 2022

might be very prevalent in increasing genomic plasticity among microbiome members.

MATERIALS AND METHODS

Bacterial strains and growth conditions

The bacterial strains, plasmids, and mobile genetic elements used in this study are listed in Table S1. *Pseudoalteromonas* and *Vibrio* strains were grown in 2216E medium (Difco) or SWLB (LB in seawater) at 30 °C unless specified otherwise. *E. coli* WM3064 was grown in LB medium containing 0.3 mM DAP (2,6-diamino-pimelic acid) at 37 °C. Kan (kanamycin, 50 μg ml^{-1}), Cm (chloramphenicol, 30 μg ml^{-1}), and Spc (spectinomycin, 100 μg ml^{-1}) were used in *E. coli*, while 15 μg ml^{-1} for Cm was used in *Pseudoalteromonas* and *Vibrio* spp. Ery (erythromycin, 15 μg ml^{-1}) was used with *Pseudoalteromonas* spp. IPTG (isopropyl-*β*-D-thiogalactopyranoside) or arabinose was used as an inducer. Plasmids and mutants for *Pseudoalteromonas* spp. were constructed following the protocols described previously [14]. Mutants for *Vibrio* spp. were constructed using the CRISPR/Cas9 system [15]. Primers used in this study are listed in Table S2. The details of plasmid and strain construction are described in Supplementary File Text S1.

Quantification of *attB* and *attP* for VPII

For VPII, *attB* and *attP* were used to indicate the excision rate and chromosomal circle formation rate of VPII after excision. We conducted real-time quantitative PCR (qPCR) assays to quantify *attB* and *attP* for VPII as previously reported [16], and chromosomal *gyrB* was used as the reference gene. To test the impact of RdfV, IntV, RdfM, and SetCD on the excision of VPII, the pRdfV-, pIntV-, pRdfM- or pSetCD-containing strains were induced with 1.0 mM IPTG for 1.5 h at an OD_{600} of 0.8–1.

Motility and biofilm assays

Swimming motility was measured using semisolid agar plates containing 0.25% agar (w/v) in 2216E medium after culturing 8–15 h at 25 °C. Crystal violet staining was used to evaluate the amount of attached biofilm in 96-well polystyrene plates or test tubes [17]. To observe the pellicles, cells were grown in quiescent cultures in test tubes containing 2216E medium for several days. Pellicles were assayed by visual inspection of the air-liquid interface of the medium, and the pellicle morphology was photographed at 36 h. Colony biofilms were grown on SWLB or blood agar plates (Huankai Microbial Sci. & Tech. Co., Ltd). Then, colony biofilms were observed and imaged after incubating for 2 days at 30 °C.

Vibrio variant screening and confirmation

To monitor biofilm formation of the *Vibrio* variants, a biofilm reporter plasmid P_{cpsA}::*lacZ* was constructed and transferred into Va43097. *Pseudoalteromonas* strains and Va43097/P_{cpsA}::*lacZ* were mixed at a 1:1 ratio. The mixtures or Va43097/P_{cpsA}::*lacZ* alone were statically incubated in 2216E medium at 30 °C. Then, overnight cocultures were plated on 2216E agar plates containing Cm and X-gal to monitor the biofilms of *Vibrio* variants. The colonies of *Vibrio* variants were restreaked, purified, and confirmed using 16S rRNA sequencing, the reporter plasmid P_{cpsA}::*lacZ* and the intact reporter module were confirmed using PCR sequencing with primers P_{cpsA}-*lacZ*-F/-R. The lost region of *Vibrio* variants V1-V3 was confirmed by RNA-sequencing combined with PCR confirmation of the internal genes and the junction sites of VPII with primer sets intV-F/-R and junction-F/-R.

Vibrio variant quantification during cell-contact or no-contact coculturing

To further investigate whether the process of VPII loss relies on cell contact, the 1:1 mixture of *Pseudoalteromonas* and Va43097/P_{cpsA}::*lacZ* or Va43097/P_{cpsA}::*lacZ* alone were spotted onto a 0.22-μm polycarbonate membrane placed on 2216E agar plates. In parallel, no-contact experiments were carried out by growing Va43097/P_{cpsA}::*lacZ* on an membrane filter placed on top of an *Pseudoalteromonas* lawn grown on 2216E agar plates, or statically cultivating Va43097/P_{cpsA}::*lacZ* in the spent medium of *Pseudoalteromonas*. All these cultures were incubated for 3 d at 30 °C. Then, the cells were diluted in seawater and plated on 2216E agar plates containing Cm and X-gal. The white colonies were counted, and the percentage of VPII loss was calculated using 48 randomly selected white colonies to check the VPII loss by PCR.

β-galactosidase activity assay

To determine the promoter activity of *cpsA* in Va43097 WT, ΔVPII and Δ*dgc137* mutants, the β-galactosidase activity of strains harboring P_{cpsA}::*lacZ* was determined by monitoring the absorbance at 420 nm using the Miller assay method [18]. To determine the effect of the *rdfM* promoter under overexpression of SetCD, the plasmid pSetCD was transformed into the *E. coli* host carrying the reporter plasmid P_{rdfM}::*lacZ*. Overnight cultures were diluted 1:100 in LB with Kan and Cm and induced with 0.5 mM IPTG at an OD_{600} of 1. The *β*-galactosidase activity was determined after induction for 1.5 h.

Phage isolation and purification

Phage vB_ValP-FGH was purified from seawater collected from Hainan Island using the double-agar layer method. First, the filtered collected seawater and the overnight culture of strain ΔVPII were mixed with the top medium and plated onto the bottom plate. The plaques appeared after culturing the plates at 30 °C for 8 h. Then, a single plaque was selected and the process was repeated twice with similar steps to purify the vB_ValP-FGH plaque. Then, the phage plaques were collected, washed with SM buffer, and filtered with 0.22 μm filters.

Phage DNA extraction and sequencing

To extract phage DNA, phage particles were prepared using a polyethylene glycol (PEG)-mediated precipitation method as previously described [19]. Briefly, phage particles in the supernatant were treated with DNase I and RNase, precipitated by adding NaCl and PEG6000, and suspended in SM buffer. Then, the phage DNA was extracted using a TIANamp Bacteria DNA Kit (Tiangen Biotech) and sequenced with the Illumina sequencing technique. The phage genome was assembled using the short-read sequencing data by Shovill v1.1.0 with default parameters (T. Seeman, https://github.com/tseemann/shovill) and annotated with the RAST server [20].

Bacterial growth

To explore the role of the fitness island VPII on the antiphage activity of Va43097, bacterial growth was determined in the presence of phage. Briefly, equal amounts of phage were mixed with Va43097 WT or ΔVPII mutant at an MOI of 1. A bacterial culture without phage was also used as a control. Growth curves of both strains were established by measuring the OD_{600} every 60 min for 6 h. The supernatant of phage lysates of Va43097 WT and ΔVPII at 4 h was collected and observed under transmission electron microscopy.

Phage production

Phage vB_ValP-FGH was serially diluted 10-fold using SM buffer, and 10 μL of each dilution was dropped onto lawns of Va43097 WT and ΔVPII. Then, the plaques were visualized after 10 h of incubation and used for calculations and imaging. The assay was repeated at least three times with two independent cultures.

RNA extraction and transcriptome sequencing

The cells of WT and variant Va43097 were cultured in 2216E liquid at 30 °C until the OD_{600} reached 0.8–1. Then, RNA extraction and transcriptome sequencing were performed as previously reported [16]. The transcriptional sequencing data of VPII genes in WT and variant Va43097 are listed in Dataset 1. The differentially expressed genes ($|\log FC| \geq 1.5$ and $p < 0.05$) of the *Vibrio* variants compared with Va43097 WT were listed in Dataset 2.

Statistics and reproducibility

Data analyses were performed using GraphPad Prism (version 7.00). The quantitative data in each experiment were analyzed by unpaired t tests for two samples and one-way ANOVA for multiple comparisons. Asterisks represent statistically significant differences (ns, (not significant); $*p < 0.05$; $**p < 0.01$; $***p < 0.001$; $****p < 0.0001$). Individual data points are plotted with lines at the mean, and error bars represent the standard deviation in each figure. Biological replicates are shown in the figure legends.

RESULTS

Coculturing of *Pseudoalteromonas* and *Vibrio* generates *Vibrio* variants

Communities are the normal mode of growth since they increase survival for many bacterial species [21, 22].

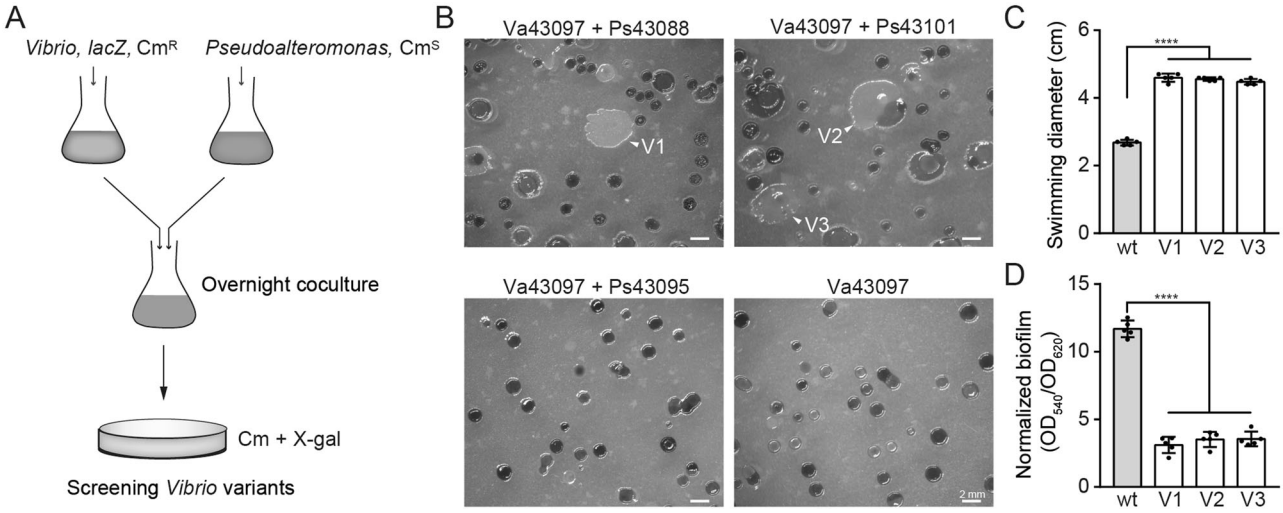

Fig. 1 Coculturing *Pseudoalteromonas* and *Vibrio* generates *Vibrio* variants with increased motility and decreased biofilm formation. **A** Schematic representation of the screening process for *Vibrio* variants. **B** Screening of *Vibrio* variants by plating the overnight coculture of Va43097 and Ps43088, Ps43101 or Ps43095 on 2216E agar plates containing Cm and X-gal. The biofilm reporter strain Va43097 P*cpsA*::*lacZ* was used in this assay, and the overnight coculture of Va43097 was also plated as a control. **C** Swimming motility of the three *Vibrio* variants was measured by culturing on semisolid agar plates for 9 h. **D** Attached biofilm of the three *Vibrio* variants was analyzed by culturing in 2216E medium for 2 h at 30 °C. *Vibrio* variants V1, V2 and V3 were selected from **B**. Individual data points are plotted with lines at the mean, and error bars represent the standard deviation. Biological replicates: WT, V1, V2 and V3, $n = 5$. Statistical analysis: Unpaired *t* test, **** indicates $p < 0.0001$.

Pseudoalteromonas spp. and *Vibrio* spp. are common, cohabiting, marine generalists, found in the gastric cavity of corals. Moreover, members of both genera are prone to forming biofilms [13, 23, 24]. To investigate the interplay between the two genera at the biofilm level, we selected several representative strains isolated from the gastric cavity of corals and performed coculture assays. We first constructed a biofilm reporter strain, *V. alginolyticus* SCSIO 43097 (abbreviated as Va43097 hereafter), by fusing a *cpsA* promoter to promoterless *lacZ* to generate the P_{cpsA}::*lacZ* plasmid. CpsA is the first gene of the capsular polysaccharide (CPS) biosynthesis cluster, and *cpsA* transcription is a proxy for biofilm formation in *Vibrio* spp; [25] therefore, this reporter plasmid can be used to indicate biofilm formation by plating cells containing this plasmid on 2216E agar plates containing X-gal. Additionally, *Vibrio* spp. containing P_{cpsA}::*lacZ* are Cm-resistant, and *Pseudoalteromonas* strains are Cm-sensitive, so *Vibrio* cells could be selected on 2216E plates with Cm after coculturing with *Pseudoalteromonas* (Fig. 1A).

When two of the *Pseudoalteromonas* strains (Ps43088 or Ps43101) were cocultured with Va43097, some larger white colonies appeared on the 2216E plates with Cm and X-gal (Fig. 1B, marked with arrows). In contrast, when cocultured with *Pseudoalteromonas* sp. SCSIO 43095 (Ps43095), most of the Va43097 colonies remained blue, and the colony morphology was similar to that of Va43097 cells grown alone on 2216E plates with Cm and X-gal. These white colonies were restreaked and purified, and they remained white on plates containing X-gal. Additionally, the survival on the Cm agar plates and PCR sequencing confirmed the presence of the reporter plasmid and intact reporter module in these white colonies (Fig. S1). Moreover, 16S rRNA gene sequencing confirmed that these were Va43097 cells. Then, the swimming motility and biofilm formation of these variants were evaluated. As shown in Fig. 1C, D, the three Va43097 variants all had higher motility but reduced biofilm formation, suggesting that genetic changes occurred in these Va43097 cells. Collectively, we demonstrated that the Va43097 variants generated during coculturing have both gained (e.g., motility) and lost (e.g., biofilm) fitness traits.

Loss of a genomic island is mainly attributed to phenotypic changes in Va43097 variants

To explore the mechanism underlying the phenotypic and genetic changes in the Va43097 variants, we conducted an RNA-seq analysis comparing the wild-type and the three variants. Surprisingly, our analysis indicated that a large 21.8 kb fragment was absent in the three Va43097 variants based on the results that expression signals from this region were not detected and the internal genes cannot be detected by PCR in the variants (Dataset 1 and Fig. 2A). Sequence analysis of the junction sites in the Va43097 variants revealed that this fragment is inserted at *trmA*, which encodes a tRNA (uridine(54)-C5)-methyltransferase in the wild-type cell. The 3′ end of *trmA* is a conserved integration hotspot for a variety of genetic elements, such as genomic islands (GIs) and prophages [26]. Our analysis revealed that this GI harbors an integrase, a recombination directionality factor (RdfV) necessary for its excision, and other hypothetical proteins. Similar GIs were found in other *Vibrio* strains, including *V. alginolyticus* strain ANC4-19 from the coral *Fungia danai* and *V. diabolicus* FDAARGOS_96 isolated from a blister *Vibrio* infection of *Homo sapiens*. No GI was integrated in this site in *V. alginolyticus* strain ATCC 33787 (Fig. 2B).

To investigate whether the loss of this GI is responsible for the phenotypic changes observed, we named this GI as VPII (*Vibrio* phenotype influencing island) and constructed the deletion mutant ΔVPII for strain Va43097. To avoid adverse effects on neighboring regions, strain ΔVPII was constructed in a way to mimic the natural excision of VPII. Briefly, we overproduced RdfV, which induces VPII excision, via pRdfV by induction with IPTG for 4 h in Va43097 cells. Next, colonies with the VPII removed were screened by PCR and further confirmed by DNA sequencing. The vector pRdfV was later cured by growing cells without adding Cm. When swimming motility was tested, the constructed deletion mutant ΔVPII showed a swimming diameter similar to that of the Va43097 variants obtained during coculturing with the *Pseudoalteromonas* strains (Fig. 2C). Similarly, the removal of VPII significantly reduced the attached biofilm formation and pellicle formation (Fig. 2D, E). Moreover, colony biofilm formation was also tested. After incubation for 2 days on the nutrient agar plates, the

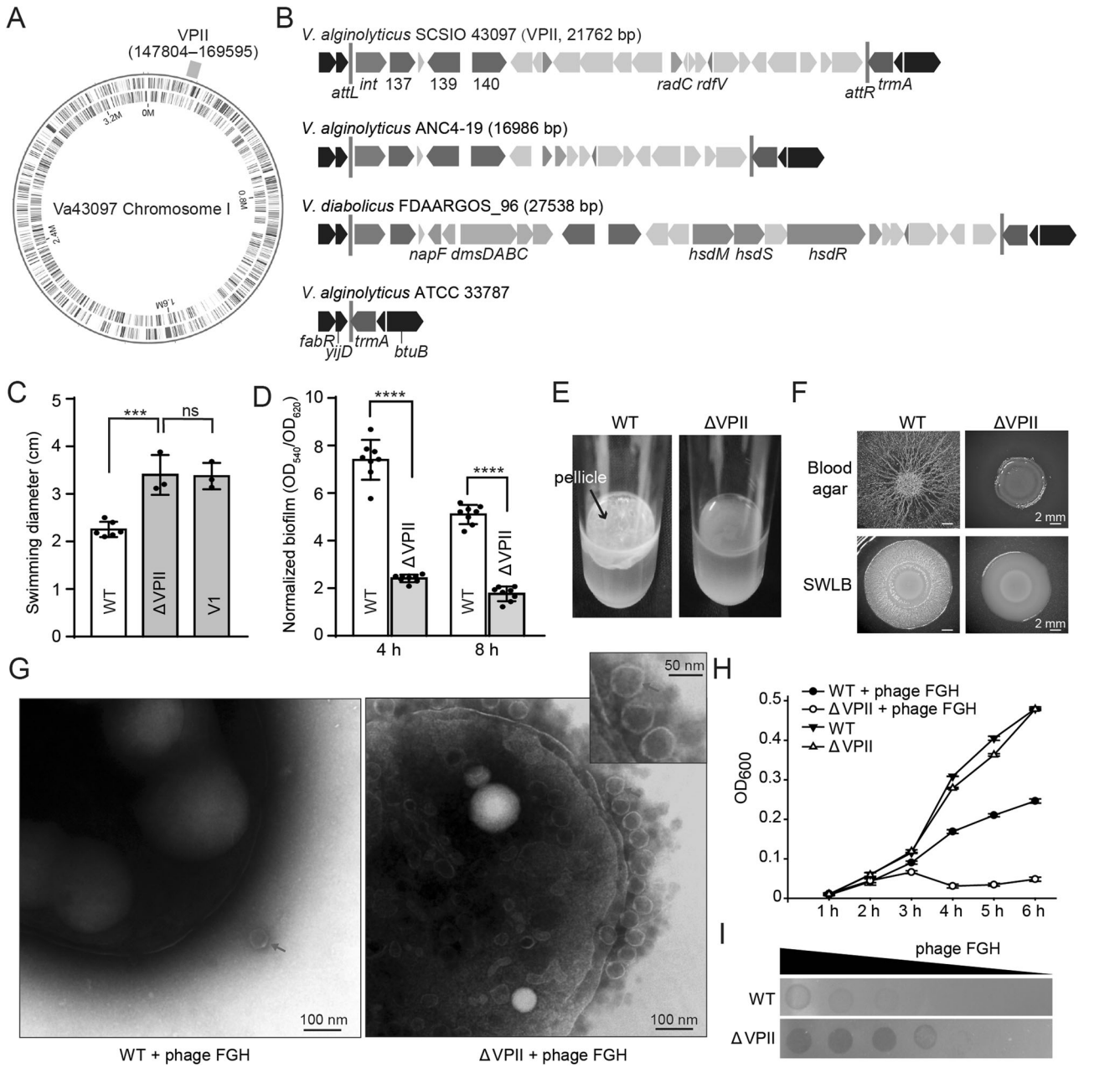

Fig. 2 Loss of the fitness island is responsible for the phenotypic changes of the Va43097 variant. A The fitness island VPII is inserted into the *trmA* gene in Va43097 chromosome I (GenBank CP071840). **B** Sequence comparison of VPII shows that highly homologous genomic islands are found in *V. diabolicus* FDAARGOS_96 (GenBank CP014094.1) and *V. alginolyticus* ANC4-19 (GenBank LTYK01000001.1). The *trmA* locus of *V. alginolyticus* ATCC 33787 was used as a reference (it contains no genomic island). Open reading frames with putative functions are shown in different colors. **C** The swimming ability of Va43097 WT, ΔVPII, and *Vibrio* variant V1 was measured by culturing on semisolid agar plates for 9 h. Individual data points are plotted with lines at the mean, and error bars represent the standard deviation. Biological replicates: WT, $n = 6$; ΔVPII, $n = 3$; and V1, $n = 3$. Statistical analysis: One-way ANOVA, *** indicates $p = 0.0005$ and ns indicates $p = 0.9991$. Biofilm formation (**D**), pellicle formation (**E**), and colony morphology (**F**) of the ΔVPII and WT strains. Individual data points are plotted with lines at the mean, and error bars represent the standard deviation. Biological replicates: WT and ΔVPII, $n = 8$. Statistical analysis: Unpaired *t*-test, **** indicates $p < 0.0001$. **G** Va43097 and ΔVPII were incubated with vB_ValP-FGH phage (FGH) (MOI = 1) for 4 h and then observed with transmission electron microscopy. Red arrows indicate phage particles. **H** Growth curve of WT and ΔVPII with or without phages. **I** Plaque formation after the phage dilutions were dropped onto Va43097 WT and ΔVPII lawns and incubated for 10 h.

rugose colony morphology disappeared when VPII was removed, suggesting that the presence of VPII increases polysaccharide production (Fig. 2F).

Since marine bacteria often encounter phages in the ocean [27], we also tested whether VPII affects phage susceptibility. When two different strains (Va43097 WT and ΔVPII) were used as hosts, we found that ΔVPII was more susceptible to some marine phages. Among them, a new phage was isolated and characterized. Transmission electron microscopy revealed phage particles having a short tail and a head with a diameter of approximately 50 nm (Fig. 2G). According to the International Committee on the Taxonomy of Viruses [28], this phage was classified as a member of the Podoviridae family and was named vB_ValP-FGH. The genome of vB_ValP-FGH (GenBank OL762410) is linear, double-

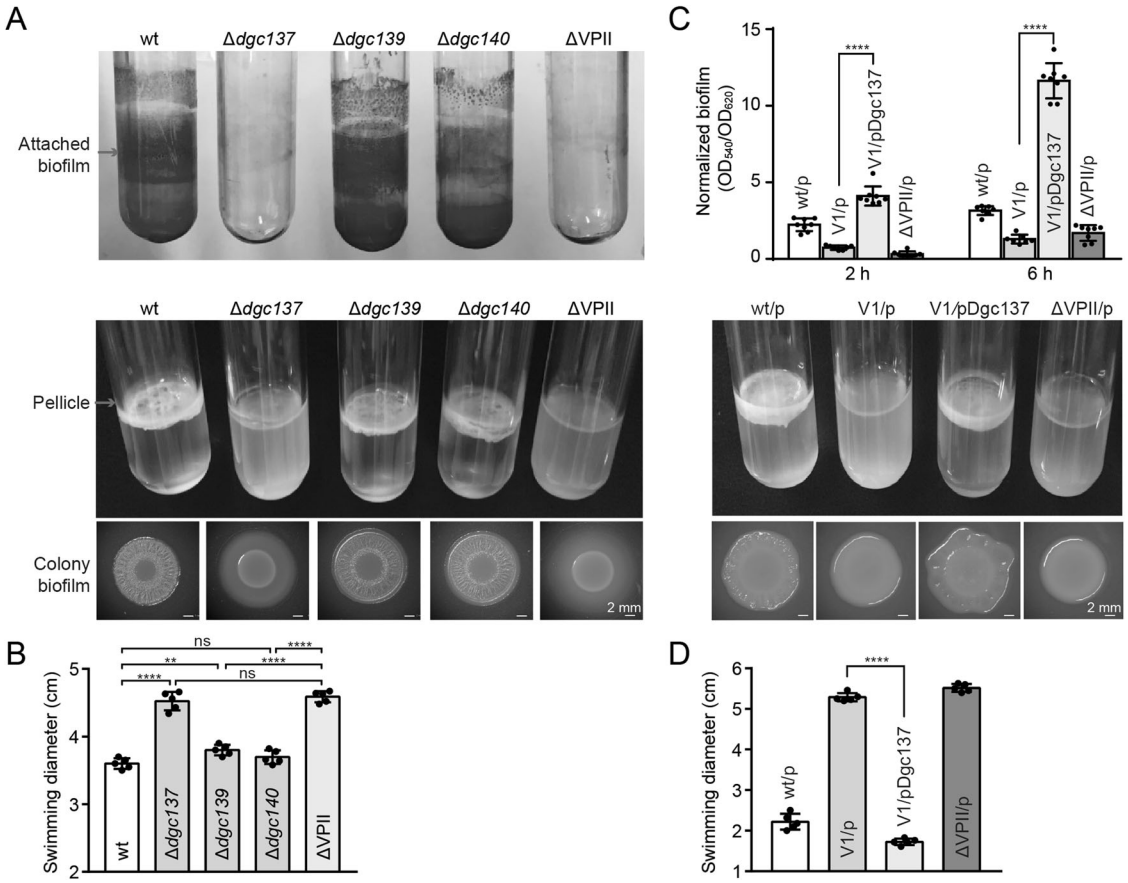

Fig. 3 Dgc137 is critical for the robust biofilm formation of Va43097. Biofilm formation **(A)** and swimming motility **(B)** of the deletion mutants Δ*dgc137*, Δ*dgc139*, and Δ*dgc140* compared with Va43097 WT. Biofilm formation (**C**) and swimming motility (**D**) after complementation of *dgc137* in *Vibrio* variant V1. wt/p (positive control), V1/p, V1/pDgc137, and ΔVPII/p (negative control) were used in the complementation experiment, and "p" indicates the empty vector pBBR1Cm. Swimming motility of the indicated strains in **B** and **D** was respectively measured on semisolid agar plates for 10 h and 15 h. Individual data points are plotted with lines at the mean, and error bars represent the standard deviation. Biological replicates in **C**: wt/p, $n = 8$; V1/p, $n = 7$; V1/pDgc137, $n = 8$; and ΔVPII/p, $n = 8$. Biological replicates in **B** and **D**, $n = 5$. Statistical analysis: Unpaired *t*-test, ** indicates $p < 0.01$, **** indicates $p < 0.0001$.

stranded DNA (36,470 bp). We identified 42 possible open reading frames (ORFs), of which 16 exhibited homology with phage-related proteins (Dataset 3). The major capsid protein shares the highest identity with P22-family phages in the UniProt virus database. Sequence analysis of the phage genome shows 80% identity (40% coverage) with *Vibrio* phage 75E35.1 and 77% identity with *Thalassomonas* phage BA3 (31% coverage).

We monitored the growth of WT and ΔVPII after the addition of vB_ValP-FGH phage in liquid culture and found that the growth of ΔVPII was dramatically inhibited, whereas the growth of WT was only moderately inhibited. No growth difference was observed between the two strains under control conditions (without vB_ValP-FGH) (Fig. 2H). In addition, using the double-agar layer method, we confirmed that the ΔVPII host is more susceptible to vB_ValP-FGH than the WT host (Fig. 2I). Using electron microscopy, we observed that more phages were attached to the surface of the ΔVPII bacterial cell than to the WT cell, suggesting that the presence of VF1-1 reduced exogeneous phage attack, possibly by decreasing phage absorption (Fig. 2G).

Dgc137 affects biofilm formation and motility by regulating c-di-GMP

To further investigate which proteins in VPII cause these phenotypic changes, we reanalyzed the sequence of VPII. Three genes next to the integrase, Dgc137, Dgc139, and Dgc140, have a putative GGDEF domain. This domain is present in diguanylate cyclase (DGC) enzymes, which synthesize cyclic diguanylate (c-di-GMP). Totally, 45 putative GGDEF-containing proteins were found in Va43097 by conserved domain search (Dataset 4). Three gene deletion mutants, Δ*dgc137*, Δ*dgc139*, and Δ*dgc140*, were constructed and verified in Va43097 (Fig. S2), and the phenotypic changes resulting from these mutations were compared to those of the ΔVPII mutant. As shown in Fig. 3A, deleting *dgc137* greatly reduced three types of biofilm formation (colony, pellicle, and attached biofilm), and the effect was equivalent to deleting all of VPII. Similarly, deleting *dgc137* increased swimming, which was equivalent to deleting all of VPII (Fig. 3B). In contrast, deleting *dgc139* or *dgc140* did not cause significant changes in biofilm formation or swimming. In addition, complementation of *dgc137* via pDgc137 in the Va43097 variant V1 rescued the wild-type biofilm and motility phenotypes, while the empty vector failed to do so (Fig. 3C, D). Collectively, these results showed that the phenotypic changes due to the loss of VPII are mainly caused by the absence of the *dgc137* gene. Furthermore, when *dgc137* was introduced into two other *V. alginolyticus* strains, it also significantly increased biofilm formation and reduced swimming (Fig. S3). These results show that the DGCs carried by mobile genetic elements can regulate biofilm formation and swimming of the host bacteria.

Since genome excision of VPII may lead to changes in neighboring regions, we also explored these areas. Sequence comparisons showed that most of the different nucleotides of *attL*

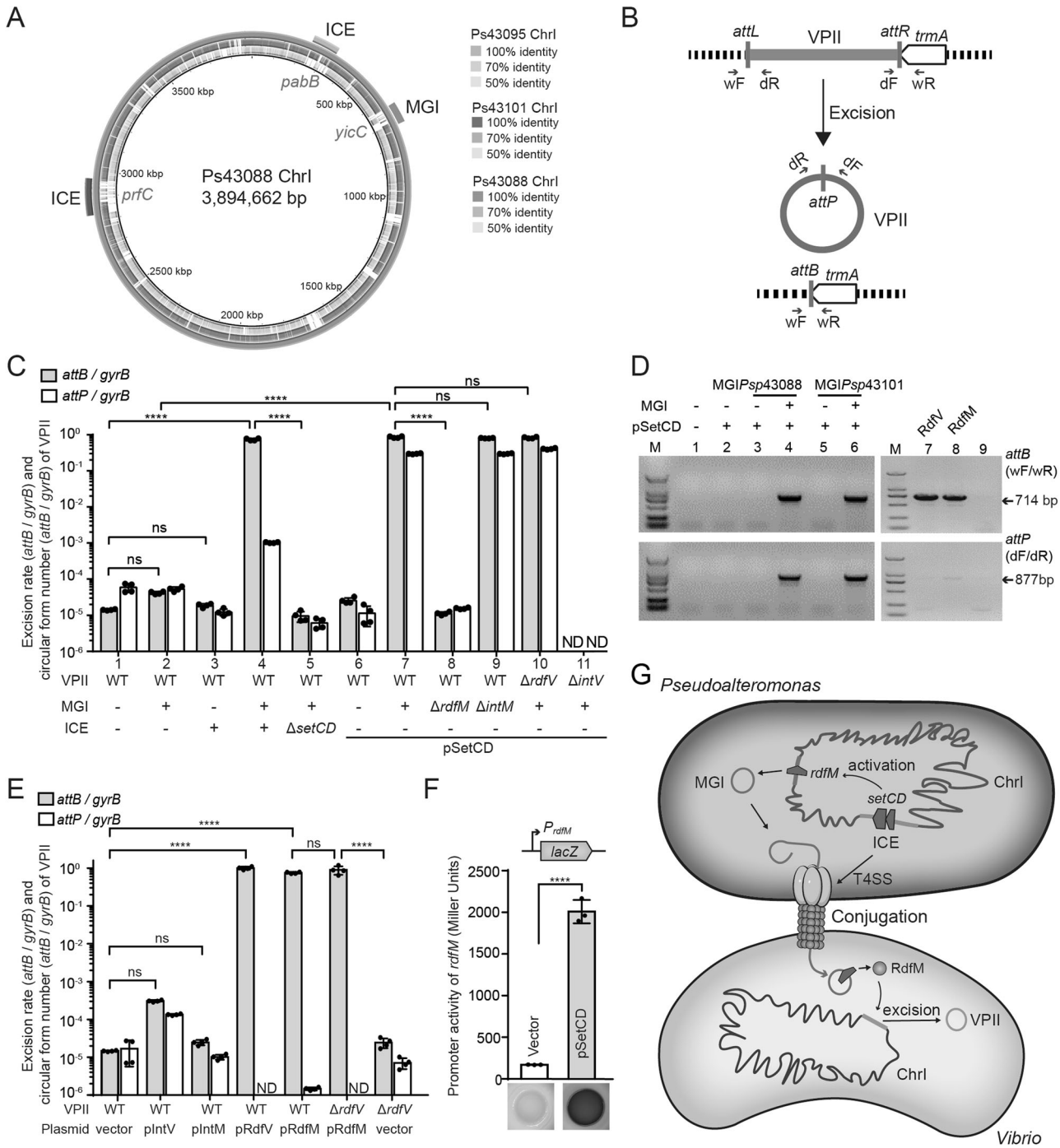

Fig. 4 VPII excision in *Vibrio* is mediated by cooperation between ICEs and MGIs from *Pseudoalteromonas*. **A** Sequence variability of the integration hotspots of chromosome I of Ps43088 (CP072675), Ps43101 (CP072673) and Ps43095 (CP087995). Ps43088 was used as reference genome. The ICEs in *prfC* and *pabB* and MGIs in *yicC* hotspots are indicated on the circle. **B** Schematic of the excision and circularization of VPII by site-specific recombination. **C** Determination of the excision frequency (*attB*) and circular form of VPII (*attP*) by qPCR in strain Va43097 harboring the derivatives of VPII, ICE, MGI or pSetCD. Individual data points are plotted with lines at the mean, and error bars represent the standard deviation. Biological replicates: group 1–10, $n = 4$; group 11, $n = 3$. Statistical analysis: One-way ANOVA, **** indicates $p < 0.0001$, and ns indicates no significant difference. ND indicates not detected. **D** The excision and circularization of VPII confirmed by PCR using primers indicated in **B**. Lane M, DL2000 marker; lanes 1–6, strain Va43097 harboring the indicated MGIs and plasmid pSetCD; strain Va43097 harboring pRdfV (lane 9), pRdfM (lane 10) or empty vector pHGECm (lane 11). **E** Determination of *attB* and *attP* by qPCR in strain Va43097 harboring the plasmids pIntV, pRdfV, pIntM or pRdfM. Individual data points are plotted with lines at the mean, and error bars represent the standard deviation. Biological replicates: $n = 4$. Statistical analysis: One-way ANOVA, **** indicates $p < 0.0001$, and ns indicates no significant difference. ND indicates not detected. **F** The promoter activity of *rdfM* was measured when SetCD was overexpressed via pSetCD compared with the vector plasmid pHGECm. Individual data points are plotted with lines at the mean, and error bars represent the standard deviation. Biological replicates: $n = 3$. Statistical analysis: Unpaired t test, **** indicates $p < 0.0001$. **G** A schematic diagram illustrates that VPII excision from *Vibrio* is mediated by ICE and MGI from *Pseudoalteromonas* after conjugation. Self-transmissible ICE mediates the excision and transfer of MGI, and MGI-encoded RdfM regulates VPII excision.

and *attR* were in the third position of a triplet codon, and only two or three amino acids at the N-terminus of TrmA were altered after excision (Fig. S4). VPII is integrated into the 3′ end of the *trmA* gene, which is replaced by the neighboring sequence of VPII after genome excision. In addition, no significant difference was found at the transcriptional level for the *trmA* gene in the wild-type and the three Va43097 variants in our above transcriptome analysis (Dataset 1). Transcriptome analysis of planktonically growing cells showed that the 172 genes were differentially expressed in Va43097 variant compared to the Va43097 wild-type strain. The *cpsA-cpsJ* genes in the CPS biosynthesis cluster were decreased significantly when VPII was lost (Dataset 2). In some *Vibrio* species, c-di-GMP regulates swimming and biofilm formation, and the *cpsA* promoter responds to changes in c-di-GMP levels [29]. Thus, the biofilm reporter P_{cpsA}::*lacZ* was used to assess the changes in intracellular c-di-GMP levels. Quantitative assays showed that the promoter activity of P_{cpsA} in the Va43097 wild-type strain was twofold higher than that in the Δ*dgc137* strain or the ΔVPII strain (Fig. S5). Collectively, these results demonstrate that DGC137 in VPII regulates swimming and biofilm formation by affecting the c-di-GMP level in host cells.

VPII excision in *V. alginolyticus* is mediated by cooperation between ICE and MGI from *Pseudoalteromonas*

Sequence analysis indicated that the junction sites in the Va43097 variants are identical to the attachment sites in the constructed ΔVPII strain (Fig. S6), suggesting that the Va43097 variants might occur through site-specific recombination. As shown above, Va43097 variants with VPII loss were only generated after coculturing Va43097 with Ps43088 or Ps43101 but not with Ps43095. Next, quantitative assays were performed to investigate whether the process of VPII loss relies on cell contact using a *lacZ* reporter system combined with PCR verification to check for VPII loss (Table S3). During co-culturing with the two *Pseudoalteromonas* strains which allow cell contact, the percentage of VPII loss in Va43097 was estimated to be 2.1 ± 1.2 % and 2.0 ± 0.6% when co-cultivated with Ps43088 and Ps43101. By contrast, when the two strains were co-cultured but separated with a membrane that circumvents conjugative transfer of mobile genetic elements, no GI loss was detected for Va43097. Consistent with this result, adding spent medium of Ps43088 or Ps43101 did not lead to VPII loss. These results suggested that the generation of GI lost variants depends on the cell-contact between Va43097 and Ps43088 or Ps43101. Since these three strains are from the same genus and share a conserved set of essential genes, we hypothesized that the difference in the mobilome of these strains may play a critical role in mediating VPII loss. Thus, we analyzed the mobile genetic elements in the genomes of Ps43088, Ps43101, and Ps43095. Three loci are considered hotspots for mobile genetic elements [30]: the *prfC* gene encoding peptide chain release factor 3, the *pabB* gene encoding para-aminobenzoate synthase component II, and the *yicC* gene encoding a putative stress-induced protein (Fig. 4A; Fig. S7). We found that there are major differences in the integrative and conjugative elements (ICEs) and mobilizable genomic islands (MGIs) present in these genomes. Both Ps43088 and Ps43101, which induce the formation of *Vibrio* variants, contain ICEs and MGIs inserted into these loci in their genomes (Fig. 4A). In contrast, no ICE or MGI was found in the genome of Ps43095. The ICEs in Ps43088 and Ps43101 contain a heterogeneous excision/integration module (*xis* and *int*) but share similar conjugation (*mobI* and *mpf* regions) and regulation modules (*setCD* and *setR* genes). Our genomic analysis revealed that these ICEs are likely self-transmissible elements belonging to the SXT/R391 family. The MGIs in Ps43088 and Ps43101 exhibited core conserved regions similar to *Vibrio* MGIs, including the excision/integration module (*rdfM* and *intM*) and origin of transfer (*oriT*). In addition, these ICEs and MGIs also harbor cargo genes encoding adaptive traits such as resistance to antibiotics and heavy metals, an RND efflux pump, toxin-antitoxin systems, and restriction-modification systems (Fig. S7).

To test the ability of these ICEs and MGIs to transfer between strains of different genera, conjugation assays were performed by using the *Pseudoalteromonas* strains as the donor and *E. coli* K-12 as the recipient. The results show that the transfer efficiency of the ICEs was ~10^{-5}, and the transfer efficiency of the MGIs was slightly higher than that of the ICEs, reaching 10^{-4} **(**Table S4**)**. We next determined whether these ICEs and MGIs in *Pseudoalteromonas* spp. mediate the excision and loss of VPII in *Vibrio* spp. Since the ICEs and MGIs in Ps43088 and Ps43101 have conserved core genes, the ICE and MGI in Ps43088 were introduced into Va43097 for further study. VPII is excised from the *Vibrio* host chromosome by recombining the *attL* and *attR* sites and generates an *attB* site (present only after VPII excision) or *attP* site (present only after the excised VPII is circularized) (Fig. 4B). We then quantified VPII excision by measuring the percentage of cells containing *attB* and *attP* sites using qPCR assays in the presence of ICE and/or MGI in strain Va43097. Our results show that the presence of ICEs or MGIs alone in Va43097 did not lead to VPII loss, while the presence of both resulted in a 71,000-fold increase in the excision rate of VPII, leading to the majority of Va43097 cells losing VPII (74 ± 0.3%) (Fig. 4C).

Next, we wanted to explore the cooperative action of ICEs and MGIs in mediating the genome excision of VPII from Va43097 in detail. We constructed several single gene deletion mutants within ICE and MGI in Va43097 to identify the key genes that mediate this process. We first deleted the conserved genes *setC* and *setD*, coding for a transcriptional regulator complex which is essential for the activation of the conjugative transfer of ICE and MGI [31]. The result showed that deletion of *setCD* abolished the excision of VPII in the presence of MGIs. Moreover, we found that overexpressing *setCD* was sufficient to induce the excision of VPII from Va43097 in the presence of MGIs, resulting in 86.00 ± 0.05% cells losing VPII (Fig. 4C). These results show that SetCD in ICEs plays an important role in VPII excision. Additionally, we also found that overexpressing *setCD* in the absence of MGIs did not lead to VPII excision, suggesting that proteins encoded by MGIs are also needed. Given that both MGIs in Ps43088 and Ps43101 excise VPII in the presence of SetCD (Fig. 4D), we hypothesized that the core genes in MGIs mediate VPII excision. Thus, we deleted the conserved gene *intM* or *rdfM*, which respectively encodes the integrase and recombination directionality factor necessary for MGI integration and excision, from strain Va43097 harboring MGI and pSetCD. The results showed that the deletion of *rdfM* but not *intM* abolished the excision of VPII in the presence of SetCD, suggesting that RdfM is the key factor in MGI mediating VPII excision (Fig. 4C). We then tested the *rdfM* gene and found that overexpressing RdfM alone resulted in VPII excision, but overexpressing IntM alone did not, suggesting that overproduction of RdfM can directly activate VPII excision (Fig. 4E, Fig. S8A).

To determine the VPII essential proteins for the site-specific recombination of VPII, we deleted the *intV* and *rdfV* genes, encoding the putative integrase and recombination directionality factor for VPII integration and excision. qPCR assays demonstrated that IntV was essential for VPII excision, but RdfV was nonessential for VPII excision when MGIs and pSetCD were present (Fig. 4C). Moreover, the production of RdfM in the Δ*rdfV* mutant resulted in VPII excision with a high frequency, similar to the production of RdfV (Fig. 4D, E). These results suggest that IntV is essential for VPII excision, but RdfV is dispensable when RfdM is present. Since MGIs alone could not induce VPII excision in strain Va43097, we then tested the possibility that SetCD in ICEs activates RdfM. Sequence analysis showed that the promoters of *rdfM* in MGI*Psp*43088 and MGI*Psp*43101 share similar SetCD binding sites from *Vibrio* MGIs near the −35 region (Fig. S8B). In addition, a *lacZ* transcriptional fusion P_{rdfM}::*lacZ* was constructed to test the promoter activity of *rdfM* by measuring *β*-galactosidase activity. When SetCD was produced via pSetCD by induction with IPTG for 1.5 h, the

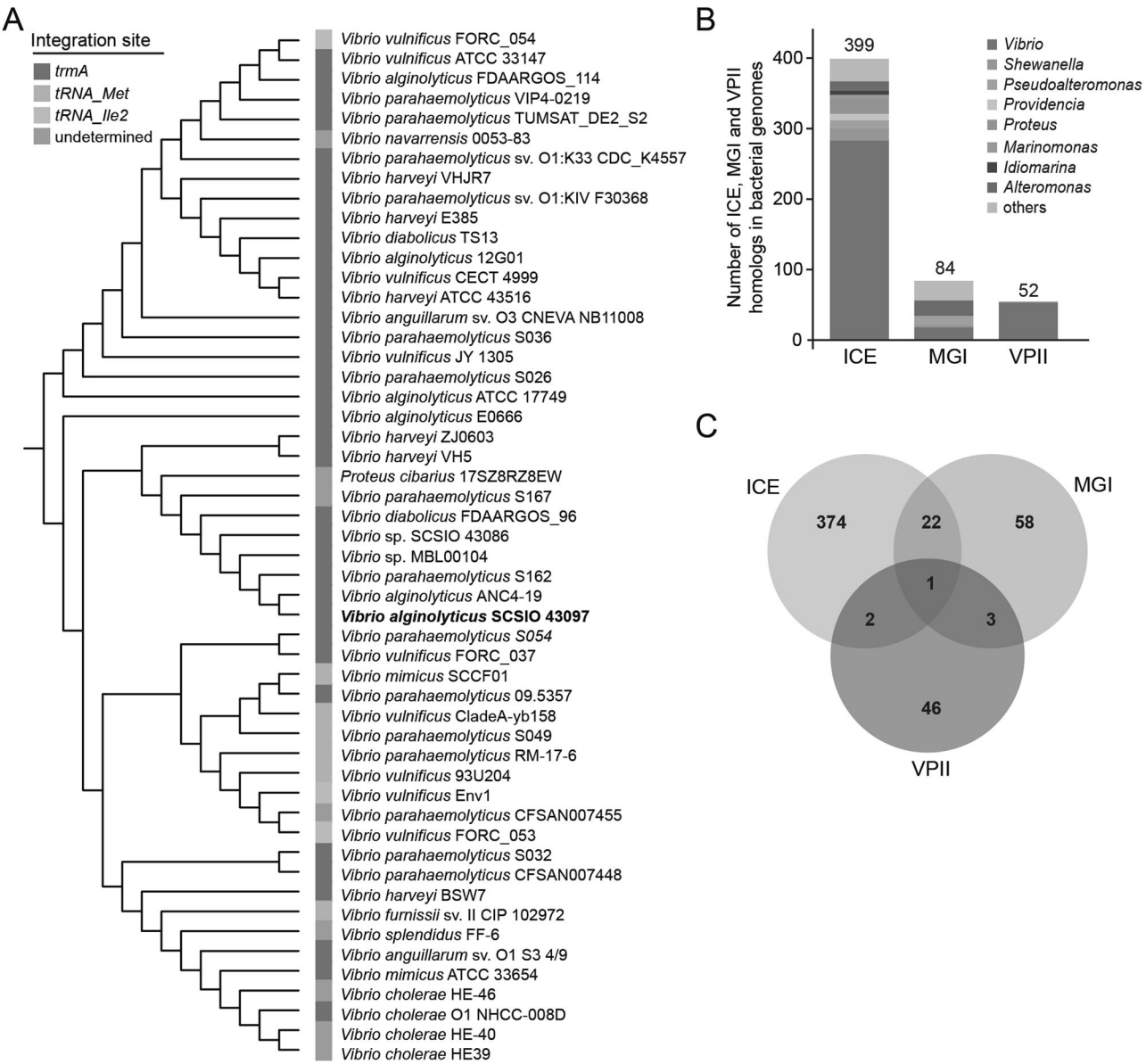

Fig. 5 Phylogenetic analysis of RdfV homologs and their cognate IntV proteins. A Neighbor-joining phylogenetic tree of RdfV in VPII and 51 homologs that show ≥83% identity with RdfV in VPII based on amino acid (aa) sequences. The integration sites of the VPII homologs are indicated with different colors. **B** Distribution of SXT/R391 ICEs, MGIs, and VPII in representative genera. **C** A Venn diagram shows the distribution of SXT/R391 ICEs, *yicC* integrated MGIs and *trmA* integrated VPII in bacterial genomes.

promoter activity of *rdfM* increased 11.8 ± 0.9-fold compared with that in the control vector (Fig. 4F). In conclusion, we demonstrated that the cooperation of SXT/R391 ICEs and MGIs mediated the loss of VPII, and RdfM in MGIs elicited VPII excision (Fig. 4G).

Cooccurrence of ICEs, MGIs, and VPII in gram-negative bacteria

To gain insights into the universality of stepwise interactions, we analyzed the distribution of SXT/R391 ICEs and MGIs in *yicC* and VPII in *trmA* (Datasets 5-7). Given a sequence-dependent interaction, 399 SXT/R391 ICEs were retrieved from the IMG/M database according to the conserved SetC protein (≥90% identities), and 85 MGIs were retrieved according to RdfM (≥90% identities). A total of 52 VPIIs were retrieved from the IMG/M database according to RdfV (≥83% identity), 51 of which were found in *Vibrio*. Moreover, 35 of the VPIIs integrated into the *trmA* gene, 9 of them were integrated into $tRNA^{Met}$ or $tRNA^{Ile2}$ (Dataset 7 and Fig. 5A). Three types of mobile genetic elements were found in *Vibrio*, *Shewanella*, *Pseudoalteromonas, Alteromonas*, and other common environmentally important genera (Fig. 5B). A Venn diagram shows that 22 bacterial genomes harbor both ICEs and MGIs, 2 genomes harbor ICEs and VPIIs, and 3 genomes harbor MGIs and VPIIs. Interestingly, the strain *Vibrio parahaemolyticus* S167 contains all three mobile genetic elements (Fig. 5C). However, the presence of all three mobile elements needs to be further verified due to the incomplete genome assembly (Dataset 7). Together, the cooccurrence of these mobile genetic elements should contribute to the creation of genetic variants of gram-negative bacteria cohabiting different niches.

DISCUSSION

The *Vibrio* genus is diverse and found in various marine environments. Here, we discovered that mobile genetic elements from a competitor drives intraspecies diversification of *Vibrio* spp. The *Vibrio* genus includes fast growers that easily become the dominant

species in environments with plentiful resources. However, the fast expansion of the dominant species may lead to a local decrease in species diversity [32, 33]. Due to the scarcity of resources in most marine environments that limit *Vibrio* overgrowth, it is critical for prokaryotic competitors to develop efficient strategies to maintain their own survival. *Pseudoalteromonas* spp. have a nutritional requirement similar to that of *Vibrio* spp [6–8]. In addition, the ability to form biofilms is critical for occupying specific metabolic niches such as the coral gastric cavity, and strains from the *Vibrio* and *Pseudoalteromonas* genera exhibit high biofilm forming abilities. Previous studies have shown that *Pseudoalteromonas* spp. can employ strategies such as the secretion of active compounds or proteolytic enzymes to compete with their *Vibrio* counterparts [9, 10, 34]. In this study, we discovered a strategy used by which the mobilome is employed by *Pseudoalteromonas* spp. to increase the genome plasticity of *Vibrio* spp. The loss of the genomic island in *Vibrio* spp. mediated by *Pseudoalteromonas* spp. leads to increased motility, which might be important for nutrient acquisition in the gastric cavity of corals [35, 36]. The fitness trade-off between planktonic and biofilm lifestyles is central for bacterial survival and can lead to the stable coexistence of genetically-distinct lineages for spatial niches.

c-di-GMP, an important second messenger in bacteria, modulates diverse cellular functions, including biofilm formation, motility, virulence, and cell division. The level of c-di-GMP is controlled by the coordination of DGCs and phosphodiesterases [37]. The complexity of c-di-GMP regulation is exemplified by the large number of genes involved in c-di-GMP metabolism; for example, there are more than 60 chromosomally encoded genes in *Vibrio cholerae* and at least 40 genes in *Pseudomonas aeruginosa* related to c-di-GMP [38, 39]. In this study, 45 putative GGDEF-containing proteins were found in Va43097. Although GGDEF domain proteins may be redundant, the role of Dgc137 in increasing biofilm formation and reducing swimming was shown. In addition, when Dgc137 was introduced into two other *V. alginolyticus* strains, it also increased biofilm formation and reduced swimming. These results show that the DGCs carried by mobile genetic elements can rewire the biological behavior of host bacteria. Our transcriptome analysis identified several genes related to biofilm formation and secondary metabolites biosynthesis that were differentially expressed when VPII is lost; hence, the pathways that are directly regulated by Dgc137 and its involvement with other GGDEF domain proteins in *V. alginolyticus* should be further investigated.

GIs can both integrate into and excise from the bacterial genome and exist in closely-related strains; they are usually flanked by short direct repeats and are often associated with tRNA genes or some other gene hotspots [40, 41]. Comparison of bacterial genomes has revealed a remarkable amount of gene acquisition and gene loss, but the dynamics and mechanisms of gene gain and loss are still incomplete. SXT/R391 ICEs are one of the most prominent GIs studied; they are self-transmissible and are distributed-widely in marine bacteria [42]. The SXT/R391 ICEs mobilize nonconjugative plasmids or MGIs in *trans* based on similar origin of transfer (*oriT*) sequences [30]. In our previous study, the SXT/R391 ICEs mediated the excision and mobilization of a defective GI after tandem integration into the ICE with the GI in *cis* [16]. In contrast, here we found that the MGI activated by SXT/R391 ICEs excised the unrelated fitness island VPII in *Vibrio* spp. These results collectively show that SXT/R391 ICEs function as major contributors to genome plasticity.

The mobilome is critical to our understanding of the movement of genes and to understanding how associated phenotypes arise via horizontal gene transfer in microbiota [43]. However, previous studies mostly focus on the function of one or two mobile genetic elements. Here, we show that tight cooperation of three different mobile genetic elements generates genetic variations. Specifically, three main components of the mobilome (ICE, GI and MGI) cooperate to manipulate genome plasticity, and our study reveals that the mobilome is a powerful molecular tool for rapidly promoting the genomic diversification of *Vibrio* species. Overall, our study cements the importance of the mobilome as a functional unit by providing new insights into the complexity of microbial interactions, including the impact of the mobilome on phage resistance, biofilm formation, and swimming motility.

DATA AVAILABILITY

The complete genome sequences of the strains Va43097, Ps43088, Ps43101, Ps43095, and phage vB_ValP-FGH have been deposited in GenBank under the accession numbers CP071840-CP071841, CP072675-CP072676, CP072673-CP072674, CP087995-CP087996, and OL762410. The transcriptome data of Va43097 and its variants can be freely accessed via the Science Data Bank at https://doi.org/10.57760/sciencedb.01844.

REFERENCES

1. Reen FJ, Almagro-Moreno S, Ussery D, Boyd EF. The genomic code: inferring Vibrionaceae niche specialization. Nat Rev Microbiol. 2006;4:697–704.
2. Thompson FL, Iida T, Swings J. Biodiversity of vibrios. Microbiol Mol Biol Rev. 2004;68:403–31.
3. Rosenberg E, Koren O, Reshef L, Efrony R, Zilber-Rosenberg I. The role of microorganisms in coral health, disease and evolution. Nat Rev Microbiol. 2007;5:355–62.
4. Neulinger SC, Jarnegren J, Ludvigsen M, Lochte K, Dullo WC. Phenotype-specific bacterial communities in the cold-water coral *Lophelia pertusa* (Scleractinia) and their implications for the coral's nutrition, health, and distribution. Appl Environ Microbiol. 2008;74:7272–85.
5. Rohwer F, Breitbart M, Jara J, Azam F, Knowlton N. Diversity of bacteria associated with the Caribbean coral *Montastraea franksi*. Coral Reefs. 2001;20:85–91.
6. Huang JF, Wu RB, Liu D, Liao BQ, Lei M, Wang M, et al. Mechanistic insight into the binding and swelling functions of prepeptidase C-terminal (PPC) domains from various bacterial proteases. Appl Environ Microbiol. 2019;85:e00611-19.
7. Paulsen SS, Strube ML, Bech PK, Gram L, Sonnenschein EC. Marine chitinolytic *Pseudoalteromonas* represents an untapped reservoir of bioactive potential. Msystems. 2019;4:e00060-19.
8. Lv XR, Li Y, Cui TQ, Sun MT, Bai FL, Li XP, et al. Bacterial community succession and volatile compound changes during fermentation of shrimp paste from Chinese Jinzhou region. Lwt-Food Sci Technol. 2020;122:108998.
9. Richards GP, Watson MA, Needleman DS, Uknalis J, Boyd EF, Fay JP. Mechanisms for *Pseudoalteromonas piscicida*-induced killing of Vibrios and other bacterial pathogens. Appl Environ Microbiol. 2017;83:e00175-17.
10. Bernbom N, Ng YY, Kjelleberg S, Harder T, Gram L. Marine bacteria from Danish coastal waters show antifouling activity against the marine fouling bacterium *Pseudoalteromonas* sp. strain S91 and zoospores of the green alga *Ulva australis* independent of bacteriocidal activity. Appl Environ Microbiol. 2011;77:8557–67.
11. Muras A, Parga A, Mayer C, Otero A. Use of quorum sensing inhibition strategies to control microfouling. Mar Drugs. 2021;19:14.
12. Shnit-Orland M, Kushmaro A. Coral mucus-associated bacteria: a possible first line of defense. FEMS Microbiol Ecol. 2009;67:371–80.
13. Rosado PM, Leite DCA, Duarte GAS, Chaloub RM, Jospin G, Nunes da Rocha U, et al. Marine probiotics: increasing coral resistance to bleaching through microbiome manipulation. ISME J. 2019;13:921–36.
14. Wang P, Yu Z, Li B, Cai X, Zeng Z, Chen X, et al. Development of an efficient conjugation-based genetic manipulation system for *Pseudoalteromonas*. Micro Cell Fact. 2015;14:11.
15. Wang P, He D, Li B, Guo Y, Wang W, Luo X, et al. Eliminating *mcr-1*-harbouring plasmids in clinical isolates using the CRISPR/Cas9 system. J Antimicrob Chemother. 2019;74:2559–65.
16. Wang P, Zeng Z, Wang W, Wen Z, Li J, Wang X. Dissemination and loss of a biofilm-related genomic island in marine *Pseudoalteromonas* mediated by integrative and conjugative elements. Environ Microbiol. 2017;19:4620–37.
17. Zeng Z, Liu X, Yao J, Guo Y, Li B, Li Y, et al. Cold adaptation regulated by cryptic prophage excision in *Shewanella oneidensis*. ISME J 2016;10:2787–800.
18. Miller JH. Experiments in molecular genetics. Cold Spring Harbor. NY: Cold Spring Harbor Laboratory Press; 1972.
19. Bertani LE, Bertani G. Preparation and characterization of temperate, non-inducible bacteriophage P2 (host: *Escherichia coli*). J Gen Virol. 1970;6:201–12.
20. Overbeek R, Olson R, Pusch GD, Olsen GJ, Davis JJ, Disz T, et al. The SEED and the rapid annotation of microbial genomes using subsystems technology (RAST). Nucleic Acids Res. 2014;42:D206–D14.
21. Flemming HC, Wingender J, Szewzyk U, Steinberg P, Rice SA, Kjelleberg S. Biofilms: an emergent form of bacterial life. Nat Rev Microbiol. 2016;14:563–75.

22. Dang H, Lovell CR. Microbial surface colonization and biofilm development in marine environments. Microbiol Mol Biol Rev. 2016;80:91–138.
23. Baker-Austin C, Oliver JD, Alam M, Ali A, Waldor MK, Qadri F, et al. *Vibrio* spp. infections. Nat Rev Dis Prim. 2018;4:8.
24. Iijima S, Washio K, Okahara R, Morikawa M. Biofilm formation and proteolytic activities of *Pseudoalteromonas* bacteria that were isolated from fish farm sediments. Micro Biotechnol. 2009;2:361–9.
25. Kimbrough JH, McCarter LL. Identification of three new GGDEF and EAL domain-containing proteins participating in the Scr surface colonization regulatory network in *Vibrio parahaemolyticus*. J Bacteriol. 2021;203:e00409-20.
26. Brenciani A, Bacciaglia A, Vignaroli C, Pugnaloni A, Varaldo PE, Giovanetti E. Phim46.1, the main *Streptococcus pyogenes* element carrying *mef(A)* and *tet(O)* genes. Antimicrob Agents Chemother. 2010;54:221–9.
27. Breitbart M, Bonnain C, Malki K, Sawaya NA. Phage puppet masters of the marine microbial realm. Nat Microbiol. 2018;3:754–66.
28. Kropinski AM, Prangishvili D, Lavigne R. Position paper: the creation of a rational scheme for the nomenclature of viruses of *Bacteria* and *Archaea*. Environ Microbiol. 2009;11:2775–7.
29. Ferreira RB, Chodur DM, Antunes LC, Trimble MJ, McCarter LL. Output targets and transcriptional regulation by a cyclic dimeric GMP-responsive circuit in the *Vibrio parahaemolyticus* Scr network. J Bacteriol. 2012;194:914–24.
30. Daccord A, Ceccarelli D, Burrus V. Integrating conjugative elements of the SXT/R391 family trigger the excision and drive the mobilization of a new class of *Vibrio* genomic islands. Mol Microbiol. 2010;78:576–88.
31. Poulin-Laprade D, Matteau D, Jacques PE, Rodrigue S, Burrus V. Transfer activation of SXT/R391 integrative and conjugative elements: unraveling the SetCD regulon. Nucleic Acids Res. 2015;43:2045–56.
32. Ghoul M, Mitri S. The ecology and evolution of microbial competition. Trends Microbiol. 2016;24:833–45.
33. Bauer MA, Kainz K, Carmona-Gutierrez D, Madeo F. Microbial wars: competition in ecological niches and within the microbiome. Micro Cell. 2018;5:215–9.
34. Yu M, Wang J, Tang K, Shi X, Wang S, Zhu WM, et al. Purification and characterization of antibacterial compounds of *Pseudoalteromonas flavipulchra* JG1. Microbiology. 2012;158:835–42.
35. Yawata Y, Cordero OX, Menolascina F, Hehemann JH, Polz MF, Stocker R. Competition-dispersal tradeoff ecologically differentiates recently speciated marine bacterioplankton populations. Proc Natl Acad Sci USA. 2014;111:5622–7.
36. Ni L, Yang S, Zhang R, Jin Z, Chen H, Conrad JC, et al. Bacteria differently deploy type-IV pili on surfaces to adapt to nutrient availability. NPJ Biofilms Microbiomes. 2016;2:15029.
37. Jenal U, Malone J. Mechanisms of cyclic-di-GMP signaling in bacteria. Annu Rev Genet. 2006;40:385–407.
38. Bordeleau E, Brouillette E, Robichaud N, Burrus V. Beyond antibiotic resistance: integrating conjugative elements of the SXT/R391 family that encode novel diguanylate cyclases participate to c-di-GMP signalling in *Vibrio cholerae*. Environ Microbiol. 2010;12:510–23.
39. Ha DG, Richman ME, O'Toole GA. Deletion mutant library for investigation of functional outputs of cyclic diguanylate metabolism in *Pseudomonas aeruginosa* PA14. Appl Environ Microbiol. 2014;80:3384–93.
40. Juhas M, van der Meer JR, Gaillard M, Harding RM, Hood DW, Crook DW. Genomic islands: tools of bacterial horizontal gene transfer and evolution. FEMS Microbiol Rev. 2009;33:376–93.
41. Dobrindt U, Hochhut B, Hentschel U, Hacker J. Genomic islands in pathogenic and environmental microorganisms. Nat Rev Microbiol. 2004;2:414–24.
42. Bioteau A, Durand R, Burrus V. Redefinition and unification of the SXT/R391 family of integrative and conjugative elements. Appl Environ Microbiol. 2018;84:e00485-18.
43. Carr VR, Shkoporov A, Hill C, Mullany P, Moyes DL. Probing the mobilome: discoveries in the dynamic microbiome. Trends Microbiol. 2021;29:158–70.

ACKNOWLEDGEMENTS

This work was supported by the Local Innovative and Research Teams Project of Guangdong Pearl River Talents Program (2019BT02Y262), the National Natural Science Foundation of China (42188102, 91951203, 31625001 and 32070175), the K. C. Wong Education Foundation (GJTD-2020-12), the Youth Innovation Promotion Association CAS (2021345 to P.W), the Guangdong Major Project of Basic and Applied Basic Research (2019B030302004), the Natural Science Foundation of Guangdong Province (2019A1515011912), the Science and Technology Planning Project of Guangzhou (202002030493) and the Key Special Project for Introduced Talents Team of Southern Marine Science and Engineering Guangdong Laboratory (Guangzhou) (GML2019ZD0407).

AUTHOR CONTRIBUTIONS

PW and XW designed the study. PW, YZ, and WW performed the experiments. PW and XW analyzed the study. SL, KT, and TL contributed new reagents/analytic tools. PW and XW wrote the paper. TKW helped edit the manuscript. All authors read and approved the final manuscript.

COMPETING INTERESTS

The authors declare no competing interests.

ADDITIONAL INFORMATION

Supplementary information The online version contains supplementary material available at https://doi.org/10.1038/s41396-022-01272-1.

Correspondence and requests for materials should be addressed to Xiaoxue Wang.

Reprints and permission information is available at http://www.nature.com/reprints

Publisher's note Springer Nature remains neutral with regard to jurisdictional claims in published maps and institutional affiliations.